UNIVERSIDAD DE CUENCA
FACULTAD DE INGENIERÍA
MAESTRÍA EN ECOHIDROLOGÍA

"Impact of rain gauge density on hydrological simulation in a small mountain catchment in southern Ecuador"

TRABAJO DE TITULACIÓN PREVIA A LA OBTENCIÓN DEL TÍTULO DE: MAGISTER EN ECOHIDROLOGÍA

AUTOR:

ADRIÁN ESTEBAN SUCOZHAÑAY CALLE
C.I. 0105103766

DIRECTOR:

ING. ROLANDO ENRIQUE CÉLLERI ALVEAR, PhD
C.I. 0602794406

CUENCA – ECUADOR

MARZO - 2018

Resumen

En lugares con alta variabilidad espacio-temporal de la precipitación, como regiones de montaña, los datos de entrada pueden ser una gran fuente de incertidumbre en la modelación hidrológica. Aquí evaluamos el impacto de la estimación de la lluvia en la modelación de escorrentía en una pequeña cuenca de páramo ubicada en el Observatorio Ecohidrológico Zhurucay (7.53 km^2) en los Andes ecuatorianos, utilizando una red de 12 pluviómetros. Primero, se analizaron ocho estructuras del modelo semi-distribuido HBV-light para seleccionar la mejor estructura que represente la escorrentía observada y sus componentes de sub-flujo. Luego, utilizamos cinco escenarios de lluvia para evaluar el impacto de la precipitación espacial en el desempeño del modelo. Finalmente, exploramos cómo un modelo calibrado con una lluvia lejos de perfecta se desempeña utilizando nuevos datos de lluvia mejorados. Si bien todas las estructuras del modelo pueden representar la escorrentía total, la estructura estándar supera a las demás al simular los componentes de sub-flujo. El desempeño del modelo mejoró al aumentar la calidad de la precipitación espacial. Tres pluviómetros distribuidos en la parte superior, media e inferior de la cuenca pudieron representar adecuadamente su precipitación media y esto se trasladó a una buena simulación de escorrentía. Finalmente, usando datos mejorados de lluvia aumento la calidad de la simulación del modelo calibrado con lluvia lejos de perfecta. Estos resultados confirman que en regiones de montaña la incertidumbre del modelo está muy relacionada con la precipitación espacial y, por lo tanto, con el número y ubicación de los pluviómetros.

Palabras clave

Modelación lluvia-escorrentía; Monitoreo de lluvia; Estimación de precipitación; Incertidumbre de modelación; Ecosistema de páramo

Abstract

In places with high spatio-temporal rainfall variability, as mountain regions, input data could be a large source of uncertainty in hydrological modelling. Here we evaluate the impact of rainfall estimation in runoff modelling in a small páramo catchment located in the Zhurucay Ecohydrological Observatory (7.53 km^2) in the Ecuadorian Andes, using a network of 12 rain gauges. First, 8 structures of the HBV-light semi-distributed model were analyzed in order to select the best model structure to represent the observed runoff and its sub-flow components. Then, we used five rainfall scenarios to evaluate the impact of spatial rainfall estimation in model performance and parameters. Finally, we explored how a model calibrated with far-from-perfect rainfall estimation would perform using new improved rainfall data. Results show that while all model structures were able to represent the overall runoff, the standard model structure outperforms the others for simulating sub-flow components. Model performance improved by increasing the quality of spatial rainfall estimation. Three rain gauges distributed in the upper, middle and lower catchment were able to represent properly the mean areal rainfall and this was translated to a good runoff simulation. Finally, improved rainfall data enhanced the runoff simulation from a model calibrated with rainfall far-from-perfect. These results confirm that in mountain regions model uncertainty is much related to spatial rainfall and, therefore, to the number and location of rain gauges.

Keywords

Rainfall-runoff modelling; Rainfall monitoring; Precipitation estimation; Modelling uncertainty; Páramo ecosystem.

Índice

Índice de figuras

Índice de tablas

Cláusula de Propiedad Intelectual

Adrián Esteban Sucozhañay Calle, autor del trabajo de titulación "Impact of rain gauge density on hydrological simulation in a small mountain catchment in southern Ecuador", certifico que todas las ideas, opiniones y contenidos expuestos en la presente investigación son de exclusiva responsabilidad de su autor.

Cuenca, 12 de marzo de 2018

Adrián Esteban Sucozhañay Calle

C.I. 0105103766

Cláusula de licencia y autorización para publicación en el Repositorio Institucional

Adrián Esteban Sucozhañay Calle en calidad de autor y titular de los derechos morales y patrimoniales del trabajo de titulación "Impact of rain gauge density on hydrological simulation in a small mountain catchment in southern Ecuador", de conformidad con el Art. 114 del CÓDIGO ORGÁNICO DE LA ECONOMÍA SOCIAL DE LOS CONOCIMIENTOS, CREATIVIDAD E INNOVACIÓN reconozco a favor de la Universidad de Cuenca una licencia gratuita, intransferible y no exclusiva para el uso no comercial de la obra, con fines estrictamente académicos.

Asimismo, autorizo a la Universidad de Cuenca para que realice la publicación de este trabajo de titulación en el repositorio institucional, de conformidad a lo dispuesto en el Art. 144 de la Ley Orgánica de Educación Superior.

Cuenca, 12 de marzo de 2018

Adrián Esteban Sucozhañay Calle

C.I. 0105103766

Agradecimientos

Esta investigación fue parte del proyecto "Identificación de los procesos hidrometereológicos que desencadenan crecidas extremas en la ciudad de Cuenca" financiado por la Dirección de Investigación (DIUC) de la Universidad de Cuenca y la Empresa Pública Municipal de Telecomunicaciones, Agua Potable, Alcantarillado y Saneamiento de Cuenca (ETAPA-EP). Este manuscrito es un resultado del Máster en Ecohidrología de UCuenca. Los autores agradecen a Johanna Orellana y la Prof. Daniela Ballari por su colaboración en el desarrollo del proyecto. Estamos agradecidos con el personal y los estudiantes que contribuyeron al monitoreo hidrometeorológico. También agradecemos a la comunidad Chumblin de Zhurucay que permitió la instalación de equipos en sus tierras.

1. Introduction

Páramo is a high-elevation Tropical Andean ecosystem located in the upper belt of the northern Andes ranging from 3000 to 4500 m a.s.l. (Sarmiento, 1986; Sarmiento et al., 2003). In southern Ecuador, it is characterized by the presence of tussock grasses, wetlands and scarce patches of *Polylepis sp*. (Pinos et al., 2016; Sklenář and Jørgensen, 1999). Like other mountain ecosystems worldwide recognized as water suppliers for downstream populations (Viviroli et al., 2007), the Andean páramo is the most important water source for Andean cities such as Quito, Bogota, Mérida and Cuenca, mainly due to the high water retention capacity of its soils and the constant precipitation it receives throughout the year (Buytaert and De Bièvre, 2012; Sarmiento, 2000). In Ecuador, it provides water for some of the most important hydropower projects such as Paute Integral (2353 MW) and Coca-Codo Sinclair (1500 MW). However, human activities such as grazing, cultivation and pine plantations can alter their normal hydrological regulation (Buytaert et al., 2005; Crespo et al., 2009). Therefore, a good understanding of páramo hydrology is critical for present and future water resources development (Célleri and Feyen, 2009).

Research on páramo hydrology is relatively new and mainly has focused on understanding hydrological processes such as evapotranspiration (Carrillo-Rojas et al., 2016; Córdova et al., 2015) and temporal and spatial variability of precipitation (Campozano et al., 2016; Padrón et al., 2015); hydrological functioning such as hydrological landscape controls (Crespo et al., 2011; Mosquera et al., 2015), water provenance and transit times (Correa et al., 2016; Mosquera et al., 2016a, 2016b) and base flow characterization (Guzmán et al., 2015); impact of land use change (Buytaert et al., 2005; Crespo et al., 2009; Ochoa-Tocachi et al., 2016); and weather and climate (Avilés et al., 2016, 2015; Flores-López et al., 2016). Nevertheless, rainfall-runoff modelling (and the uncertainties related to model structure, input data and model parameters) has still been little studied, even though it is key for hydrological applications and water resources management.

Modelling of páramo catchments has concentrated on studying the impact of land use (Buytaert et al., 2006c, 2004; Espinosa and Rivera, 2016) and hypothesis testing (Buytaert and Beven, 2011; Crespo et al., 2012). Nevertheless, given the high rainfall variability found in this region (Campozano et al., 2016; Célleri et al., 2007), that can reach volume differences of 25% in small catchments (Buytaert et al., 2006a) and the scarcity of spatio-temporal hydrometereological data, it is clear that the lack of rainfall monitoring can have a large impact on modelling (Célleri and Feyen, 2009).

Several studies have analyzed the impact of rainfall observations in model calibration and results (e.g. time to peak, peak flows, volume, performance and parameters) (Arnaud et al., 2011, 2002; Beven and Homberger, 1982; Chang et al., 2007; Chaubey et al., 1999; Obled et al., 1994). Younger et al. (2009), posit that synthetic rainfall perturbations mostly located in the upper and lower catchment induce changes in peaks and model parameters at the outlet, highlighting the importance of an adequate estimation of spatial precipitation. Faurés et al. (1995) found differences of 2 to 65% in runoff volume if just one of five rain gauges is used in a small catchment. Similar conclusion is provided by Bárdossy and Das (2008) and Xu et al. (2013), showing that the performance of runoff simulation improves and the uncertainty is reduced by increasing the number of rain gauges until a given threshold. In order to overcome this measuring problem, Berne et al. (2004), recommended spatial and temporal sampling for modelling purposes, making use of high quality and quantity of rainfall data which is in most cases difficult to obtain. Additionally, it is not possible to generalize these results to other ecosystems, mainly due to the fact that the impact of precipitation on runoff modelling will be influenced by the characteristics of the catchments and storms (Pechlivanidis et al., 2016; Syed et al., 2003).

Singh (1997), concluded that the hydrological response of a catchment is related to the spatial and temporal rainfall variability, suggesting that the quality of hydrological modelling can be related to the capacity to measure this variability. Lobligeois et al. (2014) tested this hypothesis using 181 catchments. It was found that those with higher rainfall variability needed a denser rain gauge network for improving runoff simulations. Finally, other studies have found that the quality of the model performance is indeed related to the quality of precipitation information (Anctil et al., 2006; Andréassian et al., 2004).

These studies have clearly established the importance of analyze the effect of rain gauge density for hydrological modelling (Segond et al., 2007). However, none of the studies cited previously has been carried out in mountainous regions, leaving a gap in knowledge about this topic in these areas (Girons Lopez and Seibert, 2016). Besides, it has an impact on monitoring, as scientists cannot make solid recommendations to water managers about the design of rainfall observation networks.

In this context, the objective of this study is to evaluate the impact of precipitation estimation in the hydrological simulation of a mountain catchment. For this purpose we implemented a dense rainfall network (11 rain gauges) in the Zhurucay Ecohydrological Observatory (7.53 km^2), in southern Ecuador. The semi-distributed conceptual rainfall runoff HBV-light model was chosen because has been widely used with good results in several ecosystems including mountain ecosystems (Bergström, 1992; Girons Lopez and Seibert, 2016; Plesca et al., 2012; Steele-Dunne et al., 2008) and offers a good tradeoff between the amount of information required and the spatial representation. First, we identified the best model structure to simulate total discharge and its sub-flow components (fast flow, interflow and slow flow). Secondly, we evaluated the model performance and parameter sensibility regarding six rainfall-monitoring scenarios using from 1 to 11 rain gauges. Finally, we explored one open question of Andean water managers. A common monitoring setting in mountain areas consists in having a single rain gauge station outside or in the outlet of the catchment area. Models are then calibrated using this configuration, evidently leading to low simulation efficiencies. However, as the catchment becomes more important (i.e. for water resources development), additional rain gauges are installed within the catchment. But, modelers will have to wait several years under this new monitoring system to recalibrate the model. This arises the question of how a model calibrated with a far-from-perfect rainfall estimation will perform using a new improved rainfall data, i.e. without undergoing a recalibration process. Thus, we sought an answer for this question.

2. Materials

2.1. Study area

This study was carried out in the Zhurucay Ecohydrological Observatory located in the southern Ecuadorian Andes, near the continental divide, draining to the Pacific Ocean. The observatory consists of a nested catchment of 7.53 km^2 with elevation ranging from 3400 to 3900 m a.s.l. (Figure 1). Mean annual precipitation is 1345 mm at 3780 m a.s.l. with weak seasonality. Rain mainly falls as drizzle and occurs almost daily (Padrón et al., 2015). Mean annual temperature is 6.0°C (Córdova et al., 2015). The geomorphology of the catchment is glacial U-shaped. The average slope is 17%, although slopes greater than 40% are found. The geology is compacted volcanic rock deposits formed during the last ice age (Coltorti and Ollier, 2000).

Andosols (Ah horizon) are the main soil type in Zhurucay, covering 80% of the area and commonly located in the hillslopes. These soils were formed by volcanic ash accumulation, they are black, humic, acid and rich in organic carbon and are located over a mineral horizon (C horizon) commonly rich in clay (Buytaert et al., 2006b; Quichimbo et al., 2012). Histosols (H horizon) cover the 20% remaining area and are commonly located in flat areas where geomorphology allows water accumulation. These soils were formed in wetlands are highly organic and are saturated most of the year (Buytaert and Beven, 2011).

The vegetation within the catchment is highly correlated with soil type (Mosquera et al., 2015) and is typical of páramo grasslands. Tussock grass grows in Andosols while cushion plants grow in Histosols wetlands (Ramsay and Oxley, 1997; Sklenář and Jørgensen, 1999), covering 70% and 25% of the area respectively. The remaining 5% of the area is covered by polylepis and pine forest. Due to the percentage of polylepis and pine forest is too low for each subcatchment, these vegetation covers were not included in the study. Further description of landscape characteristics are provided in Mosquera et al. (2015).

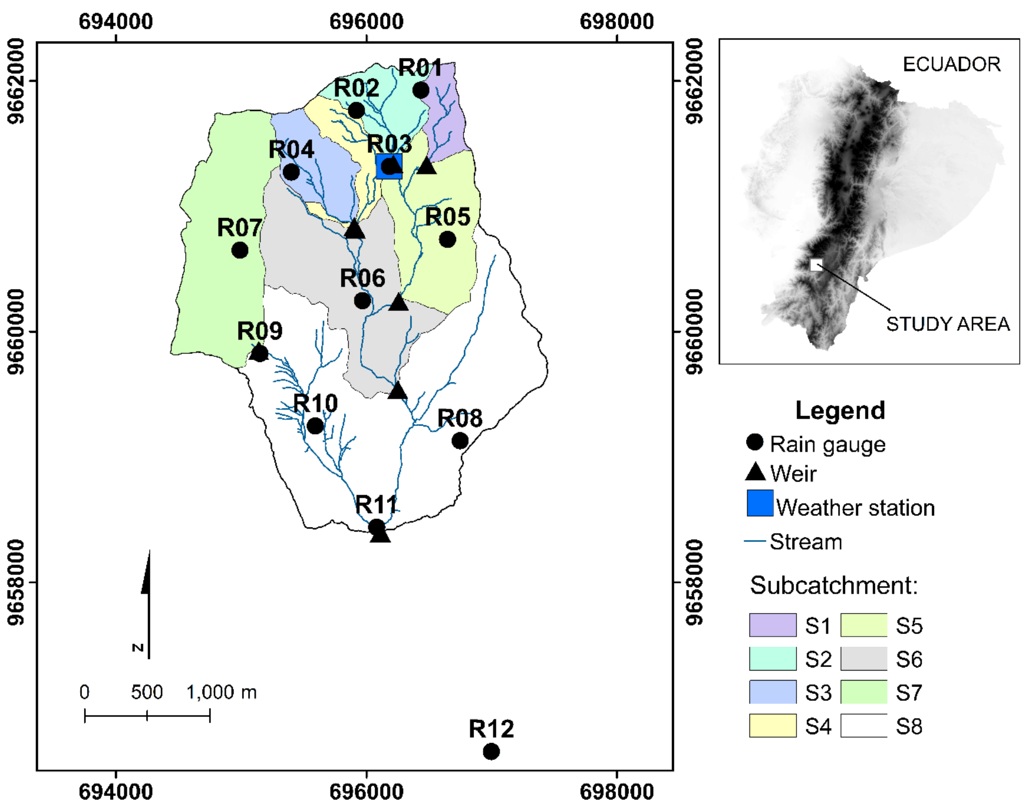

Figure 2. Study area. Coordinate system: UTM WGS84 17S.

2.2. Monitoring and data availability

The Zhurucay Ecohydrological Observatory was established in 2009 with the purpose of studying the hydrological functioning of the Andean mountain catchments. Over the years it has been equipped with two automatic meteorological stations, a laser disdrometer, several rain gauges, 10 weirs, a hillslope to study subsurface processes, and an environmental water quality monitoring system to study isotopes and metals (in soils, streams, rainfall and springs). Recent additions include an energy balance and eddy covariance system, and small-scale lysimeters.

Although Zhurucay Observatory started in 2009, the complete information of the nested weirs and five long term rain gauges started at the beginning of 2013. For this experiment the rain gauge network was complemented with a total of 12 rain gauge from 2014 to 2016. Hence, daily data of precipitation, temperature, potential evapotranspiration and runoff corresponding to the period October 2013 to October 2016 were selected for this study. These variables were used according to the requirements of the HBV-light model. Due just since 2014 was deployed the whole rain gauge network, precipitation data for the first year was obtained from five rain gauges and for the remaining years from a total of 12 rain gauges well distributed in the catchment. 11 were located inside the catchment and 1 was located 2 km downstream of the outlet. This rain gauge network is arguably the denser network in the Andes mountains at this spatial scale (1.46 rain gauges per km^2). Temperature and meteorological variables to estimate potential evapotranspiration were acquired from a weather station at 3780 m a.s.l. Runoff data was obtained from V-notch weirs at the outlet of seven subcatchments (S1 to S7) and from one rectangular weir at the outlet of Zhurucay catchment (S8) which is the focus of this study. Figure 1 shows the distribution of sensors and subcatchments. Subcatchments area and vegetation cover is presented in Table 1 which was provided by Mosquera et al. (2015).

Table 5. Subcatchment area and vegetation cover.

Subcatchment	**Area (Km^2)**	**Vegetation cover (%)**	
		Wetland	Tussock grass
S1	0.20	15	85
S2	0.38	13	87
S3	0.38	18	82
S4	0.65	18	82
S5	1.40	17	83
S6	3.28	24	76
S7	1.22	65	35
S8	7.53	25	75

2.3. HBV-light model

The HBV-light model (Seibert, 1997) is a semi distributed conceptual rainfall-runoff model and is based on the original HBV model developed by Bergström (1976) and Bergström (1992) at the Swedish Meteorological and Hydrological Institute (SMHI). This model can be distributed into different elevation and vegetation zones as well as subcatchments. HBV-light uses four routines to simulate runoff: (i) the snow routine represents snow accumulation and snow melt; (ii) the soil routine describes ground water recharge and actual evaporation as function of water storage for each elevation or vegetation zone; (iii) the response routine computes the runoff as function of water stored in reservoirs; and (iv) the routing routine simulate the routing of the runoff to the outlet of the catchment by a triangular weighting function. A detailed description of the model can be found in Seibert and Vis (2012).

The standard model consists of two serial reservoirs that receive water from the semi distributed soil routine. Storage in the upper soil reservoir (SUZ) simulates fast flow and interflow, representing the near surface and subsurface flow, respectively; while storage in the lower soil reservoir (SLZ) simulates slow flow, representing base flow. Both reservoirs are connected by a percolation rate. In total, HBV-light offers 11 different structures of reservoirs varying from one to three reservoirs with different degree of spatial distribution according to elevation and vegetation zones. Further details of model structures are found in Uhlenbrook et al. (1999). For this study the Zhurucay catchment was divided into eight subcatchments and two vegetation zones representing tussock grasses (grassland) and cushion plants (wetlands). Structures related to snow and very slow flow were not used since Zhurucay does not receive snow. Eight model structures were used in this study, as presented in Table 2.

Table 6. HBV-light model structures.

ID	Structure[a]
M1	Two boxes. SUZ and SLZ. (Standard).
M2	Two boxes. UZL threshold.
M3	Two boxes. SUZ distributed. UZL threshold.
M4	Two boxes. SUZ distributed. UZL threshold.
M5	Three boxes. STZ, SUZ and SLZ.
M6	Three boxes. STZ distributed.
M7	Three boxes. STZ and SUZ distributed.
M8	One box. UZL and PERC thresholds.

[a] STZ = Storage in top zone; SUZ = Storage in upper zone; SLZ = Storage in lower zone; UZL = Threshold parameter above which produce overland flow; PERC = Threshold parameter above which produce inter flow.

3. Methodology

First, we calibrated and validated each model structure using all rain gauges located inside the catchment. Each model structure was evaluated and compared according to the ability to simulate total runoff and its sub-flow components in order to select the model structure with the highest performance. Then, the model structure selected previously was calibrated and validated using six rainfall monitoring scenarios to evaluate the impact of rainfall estimation on the simulated runoff and parameters. Finally, the calibrated parameters with the worst rainfall scenario were employed to run the model with the remaining scenarios to analyze the possibility to enhance runoff simulation by improving rainfall information. The methodological details are explained in the following subsections.

3.1. Model calibration and validation

The HBV-light model was calibrated with three years of daily data (Oct 2013 – Oct 2016) using the standard split sample model calibration procedure (Ewen and Parkin, 1996; Klemeš, 1986) . The first, second and third year of data was used for model warming up, calibration and validation, respectively. For warming up period rainfall was estimated from 5 rain gauges (R03, R06, R07, R08 and R12) interpolated by inverse distance weighting (IDW). This interpolation method was used due to the reduced rain gauge available. For calibration and validation period rainfall was estimated from 11 rain gauges located inside the catchment interpolated by ordinary Kriging. Potential evapotranspiration was estimated by the Penman-Monteith method (Allen et al., 1998) which has been used previously in the Zhurucay observatory (Córdova et al., 2015).

The Monte Carlo procedure established by HBV-light model was used to select an optimal parameter set after performing 10,000 simulations. Table 3 lists all parameters used and their calibration range. Parameter sets were generated using random numbers from a uniform distribution. Recession coefficient for fast flow (K0) was no calibrated and was set to 0.99 d^{-1} (close to one day). Interflow (K1) and slow flow (K2) coefficients were calibrated between relative fast ranges. These considerations were taken due to the fast recession observed in these subcatchments. The simulation results for each set of parameters in the Monte Carlo procedure were optimized with Nash-Sutcliffe efficiency (NSeff) (Nash and Sutcliffe, 1970) as objective function.

Table 7. HBV-light model parameters and their range used in the Monte Carlo procedure.

Parameter	Description	Unit	Minimum	Maximum
Soil routine[a]				
FC	Maximum soil moisture	mm	250	400
LP	Soil moisture (MS) above which actual evapotranspiration reaches potential evapotranspiration (MS/FC)	-	0.5	1
BETA	Relative contribution to runoff from rain or snowmelt	-	1	3
Response routine				
K0[b]	Recession coefficient for quick flow	d^{-1}	0.999	0.999
K1	Recession coefficient for interflow	d^{-1}	0.33	0.999
K2	Recession coefficient for base flow	d^{-1}	0.066	0.2
ALPHA[c]	Non-linearity coefficient	-	0	1
UZL[d]	Threshold parameter for K0 outflow	mm	0	30
PERC[e]	Percolation from SUZ to SLZ	mm d^{-1}	0	2
UZL[f]	Percolation from STZ to SUZ	mm d^{-1}	0	30
PERC[g]	Threshold parameter for K1 outflow	mm	0	2
Routing routine				
MAXBAS	Length of triangular weighting function	d	1	1.5

[a] Parameters for each vegetation cover

[b] Parameter used only for structures M2, M4, M5, M6, M7 and M8
[c] Parameter used only for structures M1 and M3
[d] Parameter used only for structures M2, M4 and M8
[e] Parameter used only for structures M1, M2, M3, M4,M5,M6 and M7
[f] Parameter used only for structures M5, M6 and M7
[g] Parameter used only for structure M8

3.2. Evaluation of model structures

Model structures were evaluated in two steps. First, for each model structure HVB-light was calibrated and validated based on NSeff. Nevertheless, other performance indexes such as Nash-Sutcliffe efficiency with logarithms (Log NSeff), coefficient of determination (R^2) and percentage annual difference (%ADiff) were additionally calculated to provide more information about the quality of the simulation (Krause et al., 2005; Legates and McCabe Jr., 1999).

Second, to identify the most behavioral models, the simulated runoff generated from the different storages of the model structures (i.e. STZ, SUZ, SLZ) representing fast flow (FF), interflow (IF), and slow flow (SF) were compared to the flow components derived from measured runoff using the Water Engineering Time Series PROcessing tool (WETSPRO) (Willems, 2009). WETSPRO is Excel-based tool which allows separate the time series of a measured river flow in its sub-flow components in function of a recession constant (*K*) and the average fraction of each sub-flow component over the total flow (*w*). Since model structures M1 and M3 simulate only two flow components, i.e. slow flow and the combination of inter flow and fast flow, WETSPRO-derived interflow and fast flow were combined for an adequate comparison.

3.3. Rainfall monitoring scenarios

It has been selected six rainfall monitoring scenarios. These scenarios range from all the network to a single rain gauge located outside the catchment and are described in Table 4. The first scenario uses 11 rain gauge inside the catchment and therefore provides the best rainfall estimation (used in section 3.1), denominated E0. The remaining five monitoring scenarios (E1–E5), are: one configuration using three rain gauges located in the upper, middle and lower catchment (R01, R03 and R11) and four configurations using only one rain gauge in each one, located in the upper (R01), middle (R03), lower (R11) and outside the catchment (R12). For scenarios based on one single rain gauge, areal rainfall was considered uniform all over the catchment. For the three-rain-gauge scenario, areal rainfall was interpolated by inverse distance weighting (IDW). This method was selected rather than ordinary kriging due the low rain gauge density. These five scenarios were selected due it is a common practice for water managements in these areas.

Table 8. Rainfall monitoring scenarios.

ID	Rain gauge	Areal rainfall estimation method
E0	R01 to R11	Ordinary Kriging
E1	R01, R03, R11	IDW
E2	R01	Punctual
E3	R03	Punctual
E4	R11	Punctual
E5	R12	Punctual

3.4. Evaluation of the estimated rainfall from rainfall monitoring scenarios

The capacity of the estimated rainfall from monitoring scenarios E1 to E5 to represent the areal rainfall of the catchment were compared with the monitoring scenario E0 which is the best rainfall estimation, by an analysis of scatter plot, R^2 and Goodness of Rainfall Estimation index (GORE) (Andréassian et al., 2004). GORE was used to quantify the quality of the estimated rainfall time distribution. GORE is the transposition of NSeff in the precipitation domain, using the square root of the rainfall data to reduce the weight of extreme events and is expressed as:

$$GORE = 1 - \frac{\sum_{i=1}^{n}(\sqrt{P_i^E} - \sqrt{P_i})^2}{\sum_{i=1}^{n}(\sqrt{P_i} - \overline{\sqrt{P}})^2} \qquad (1)$$

where, *n* is the number of time steps of the period, P^E is the estimated rainfall from rainfall monitoring scenario and P is the best estimated rainfall available considered as reference.

3.5. Evaluation of the impact of rainfall estimation on model calibration

To evaluate the effect of the reduction of precipitation information by operating a sparse precipitation network on hydrological simulation, the HBV-light structure selected in section 3.2 was calibrated and validated using each of the rainfall scenarios in section 3.3. The performance of the simulated runoff (using NSeff) and calibrated parameters were related to the quality of the estimated rainfall (GORE) used to run the model.

Besides this, BALANCE index was used to quantify the overestimation or underestimation of the estimated rainfall total depth (Andréassian et al., 2004). BALANCE index is greater than 1 in the case of rainfall overestimation and smaller than 1 in the case of underestimation, and is expressed as:

$$BALANCE\ index = \frac{\sum_{i=1}^{n} P_i^E}{\sum_{i=1}^{n} P_i} \qquad (2)$$

3.6. Effect of improved rainfall estimation on a model calibrated with scarce data

For this objective, the model calibrated with the worst rainfall scenario (section 3.5) was run with the remaining rainfall scenarios in a step-wise fashion, i.e. by improving the spatial rainfall estimation step-by-step up to the reference scenario (E0). Then, the performances of runoff simulations (NSeff index) were analyzed regarding the quality of rainfall information (GORE index) used to run the model.

4. Results and Discussion

4.1. Evaluation of the model structures

The performances of the eight model structures, for each subcatchment and for calibration and validation periods are shown in Figure 2. As we can observe, each line represent a model structure and the overlapping of these lines indicates that all model structures present similar results. From the magnitudes of NSeff, LogNSeff, R^2 and %ADiff, it is hard to identify a model structure that outperforms the others, as there is little difference among structures. A similar result was found by Uhlenbrook et al. (1999) using six structures of HBV model in a mountainous catchment in Germany. This suggests that model parameters compensate the differences among structures. Additionally, similar results are observed for all subcatchments, which can be explained by two reasons: first, the reason explained previously and second, that physical differences between subcatchments are not large enough to produce an impact in specific model structures (Seibert, 1999).

For the catchment S8, which is the outlet of Zhurucay catchment and the focus of this study, NSeff values from eight structures vary between 0.80 to 0.83 and 0.68 to 0.73 for calibration and validation, respectively. These results were similar than the ones obtained by Buytaert and Beven (2011) in another páramo catchment of 2.53 km^2 with similar vegetation cover and altitude. Combining these NSeff values with high R^2 values (over 0.82), one might consider that the eight structures can represent the overall runoff dynamics. However, lower values of LogNSeff compared to NSeff suggest that structures may have problems to simulate low flows (Krause et al., 2005). Therefore, we compared the observed and simulated sub-flow components for each model structure. This was done for the S8 catchment and the average of S1 to S8 (Table 5).

The average of NSeff for all subcatchments shows low values for slow flow (SF) and fast flow (FF) below 0.37 and 0.20, respectively. For most of the structures NSeff values show large variability between subcatchments, e.g. for the structure M2 it was found a max value of 0.52 and a min value of -0.01 for SF. This shows that while parameters compensate the overall performance of a model structure, the simulated sub-flow components do not represent the physical functioning of the catchments, and therefore these models are not behavioral (Gupta et al., 2006).

For catchment S8 the eight structures present similar results ranging from 0.17 to 0.42, 0.48 to 0.70 and 0.65 to 0.72 for SF, IF and FF, respectively. These results indicate that SF was difficult to simulate; indeed all model structures had NSeff values below 0.42 for this sub-flow. M1 was the model structure that obtained the highest performances (0.42 SF and 0.70 IF). Therefore, M1 structure with two reservoirs that simulate slow flow and the combination of interflow and fast flow was chosen for the remaining of the study. The fact that the simplest structure has the best performance in simulating all sub-flows is because hydrologically the páramo ecosystem is relatively simple (Mosquera et al., 2015) and that its water storage-release processes is mainly controlled by water moving laterally through the organic soils to the streams (Mosquera et al., 2016a). Thus, a two-reservoir model structure represent well the hydrology of the catchment.

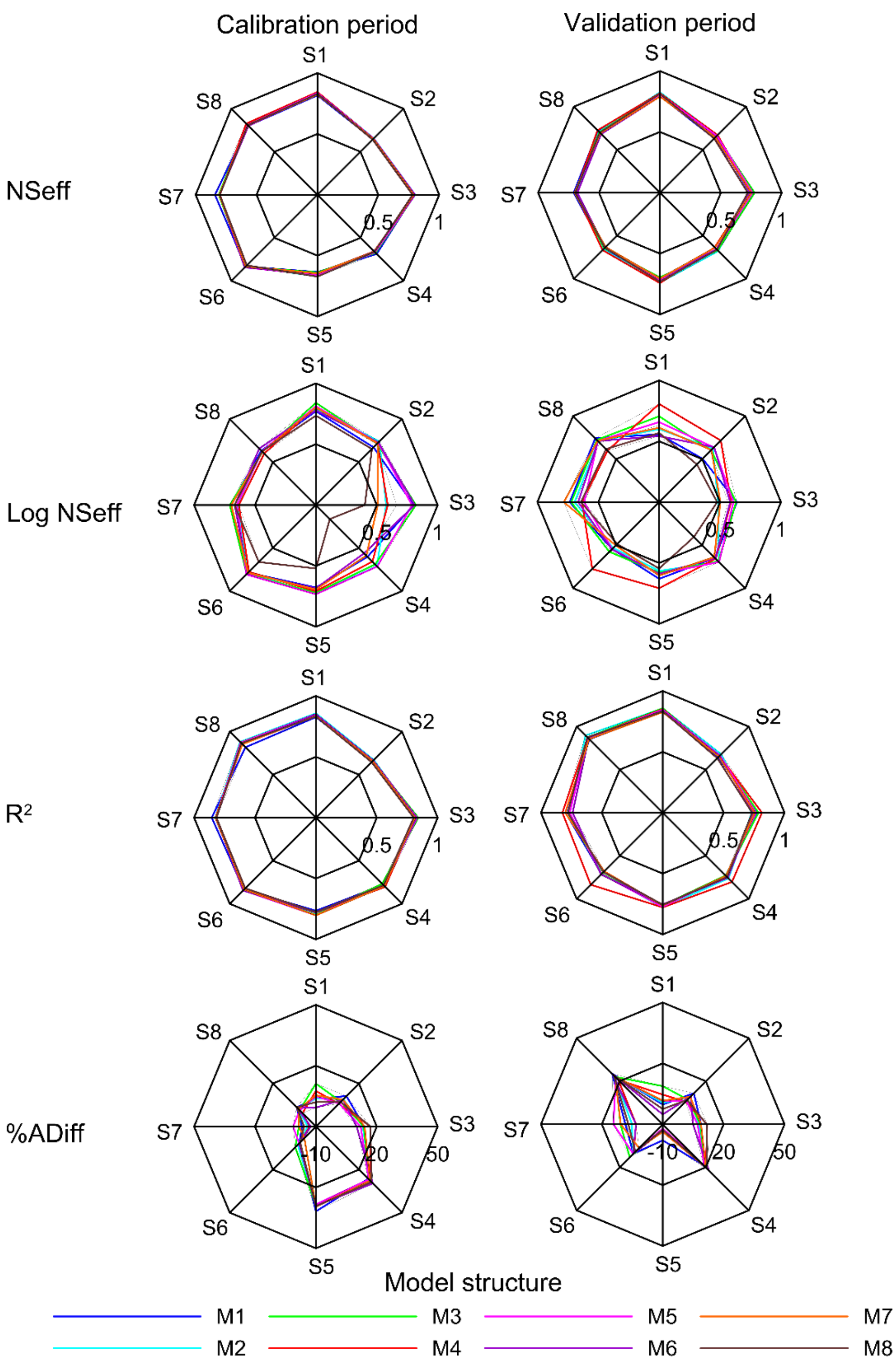

Figure 2: Performance indexes for simulated runoff. Left column for calibration period and right column for validation period. Each axis represent a subcatchment and each line represent a model structure.

Table 5: Nash-Sutcliffe efficiency for simulated flow components from each model structure. For outlet subcatchment S8 and the average of S1 to S8.

Model structure	Flow components S8			Average flow component (S1 - S8)		
	SF	IF	FF	SF	IF	FF
M1	0.42	0.70		0.32	0.72	
M2	0.17	0.68	0.67	0.07	0.61	0.08
M3	0.33	0.67		0.37	0.71	
M4	0.28	0.64	0.72	0.13	0.60	0.27
M5	0.39	0.48	0.66	0.27	0.52	0.16
M6	0.35	0.53	0.65	0.05	0.55	0.20
M7	0.36	0.62	0.66	0.19	0.55	0.09
M8	0.31	0.63	0.70	0.05	0.60	0.30

4.2. Evaluation of the estimated rainfall from rainfall monitoring scenarios

The comparison of the daily rainfall estimated from the five monitoring scenarios (E1 – E5) against the best rainfall estimation for the catchment (E0) is shown in Figure 3. It is observed that the scenario E1 using three rain gauges distributed in the upper, middle and lower catchment represents well the areal rainfall. For scenarios that use only one rain gauge to represent the areal rainfall, the position with the best representation was the middle (E3). This result is similar to Hrachowitz and Weiler (2011), suggesting that the rainfall of the middle of the catchment is similar to the average of the rainfall of all the catchment. On the other hand, it is observed that a rain gauge located in the upper catchment (E3) have better results than a rain gauge located in the lower catchment (E4). Using rainfall observations at the catchment outlet (E4) the quality of the estimation is reduced significantly, and when a single rain gauge at 2 km downstream of the outlet (E5) is used, the estimation is very different, increasing the scatter and overestimation. This shows that in this mountain setting there is a large rainfall variability at short distances, which is in line with results found by Buytaert et al. (2006a) who found that páramo rainfall can be highly variable, even at short distances of 4 km, suggesting a strong orographic influence in rainfall.

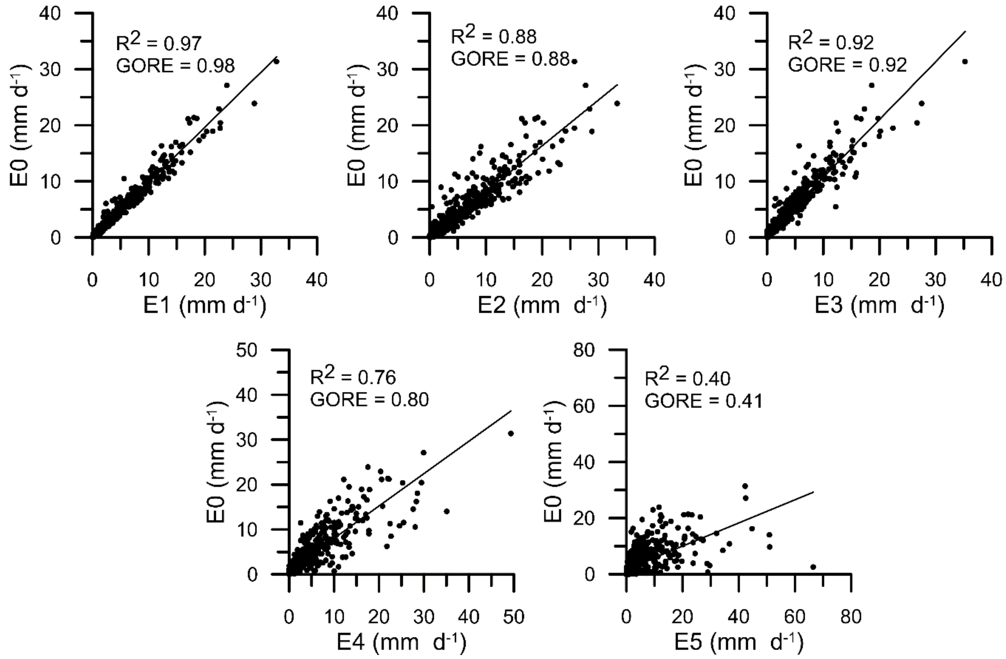

Figure 3: Scatter plot, determination coefficient (R^2) and GORE of the estimated areal rainfall of catchment S8 from monitoring scenarios E1 - E5 (axis X) against the reference estimated rainfall from monitoring scenario E0 (axis Y).

4.3. Evaluation of the impact of rainfall estimation on hydrological simulation

The impact of the rainfall estimation from the six monitoring scenarios (one being the best spatial estimation) on the performance of the simulated runoff is showed in Figure 4. This figure shows the model performance (NSeff) against the rainfall scenario (Figure 4a), the quality of the estimated rainfall (GORE, Figure 4b), and the over or under estimation of rainfall (Balance index, Figure 4c).

In Figure 4a shows that rainfall scenarios E0 and E1 produce very similar, good results, for both calibration and validation periods. This corroborate that the good rainfall quality of scenario E1 identified in section 4.2, is also translated to a good runoff simulation. On the other hand, and as expected, the rainfall scenario with the worst rainfall quality (E5) produces the poorest runoff simulation (below 0.31 NSeff). This result shows how inadequate rainfall monitoring can produce high modelling uncertainty (Chang et al., 2007). Model performance using rainfall scenarios with one rain gauge see a deterioration in NSeff values compared to best spatial rainfall. While the validation period seems satisfactory (for E2 and E3), the efficiency in the calibration period is significantly reduced.

These results also prove that there is a direct relation between the rainfall quality (GORE) and the simulated runoff performance (NSeff), as can be seen in Figure 4b. Additionally, we can observe that the slope of this relation is very pronounced, indicating that a slight reduction in the quality of the estimated rainfall can produce a big reduction in the performance of the runoff simulation. This relation was also found in some Mediterranean catchments in France (Anctil et al., 2006; Andréassian et al., 2004). Nevertheless, the slope found in this study was more pronounced compared to results of Andréassian et al. (2004), which suggests a stronger influence of the quality of rainfall input in the runoff simulation in this páramo catchment.

Finally, according to results of Andréassian et al. (2004) it was expected that the performance of runoff simulation would increase while the Balance index get closer to 1. Nevertheless, below a threshold of 0.7 it is observed random values of NSeff (Figure 4c), e.g. for a balance value of 1.11 correspond a NSeff value of 0.31 and for and higher balance value of 1.19 correspond a NSeff value of 0.63. Hence, is difficult to obtain a clear conclusion in function of the Balance index, although, the highest performance of the simulated runoff was obtained when the over or under estimation of rainfall was minimal.

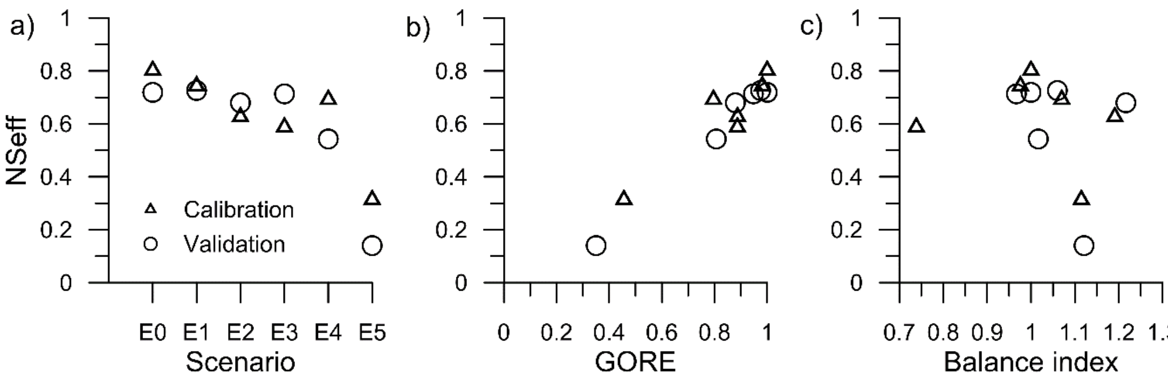

Figure 4: Impact of rainfall quality on model performance (NSeff) against: a) rainfall monitoring scenario, b) GORE index and c) Balance index. For calibration and validation period.

The sensibility of model parameters to rainfall quality is shown in Figure 5. ALPHA and BETA parameters are plotted against the GORE index. These two parameters were selected to illustrate its sensibility to rainfall quality.

The only parameter sensible to rainfall quality was ALPHA (Figure 5a). In the study of Andréassian et al. (2004), the sensibility is expressed as the reduction of the variability of the parameter values as the rainfall quality increases until reaching an optimal parameter value. In this this study was found that the higher the GORE, the higher the ALPHA. On the other hand, Figure 5b shows BETA as example of a parameter showing no sensibility to rainfall quality. In contrast of Andréassian et al. (2004) findings, here it was found that the majority of parameters are not sensible to rainfall quality. This may be caused by the relative high number of parameters which allows an over adjustment to the input data compared to the 3 and 6 parameters used in Andréassian et al. (2004). Nevertheless, at least one parameter was found sensible, showing that despite this situation, rainfall quality may still have an impact in parametrization. Therefore, it is possible that this one sensible parameter may cause the majority of the impact in the overall model performance. This can be due to a correct estimation of precipitation allows a better description of ALPHA parameter (which controls the amount of water that recharges the streams) to adapt to the high water recharge of these soils.

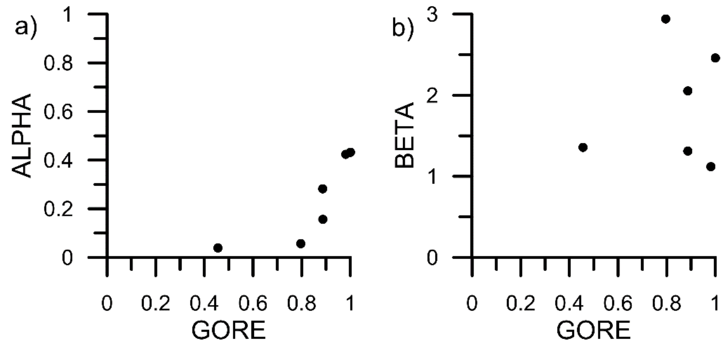

Figure 5: Sensibility of model parameters to rainfall quality (GORE). a) For a parameter sensible, ALPHA and b) for a parameter no sensible, BETA.

4.4. Effect of rainfall estimation in calibrated model

In this section, we analyzed the performance of the runoff simulation obtained from a calibrated model with far-from-perfect rainfall using new improved rainfall estimations. In this way, the model calibrated with rainfall from scenario E5 was run for the validation period with the remaining scenarios. Figure 6 shows the NSeff index from simulated runoff against the rainfall monitoring scenario and the GORE index.

Rainfall scenarios E4 to E0 produce a considerably better runoff simulation compared to scenario E5 (Figure 6a). Furthermore, NSeff values obtained from these scenarios were very similar and increased to 0.49-0.60 from an original value of 0.14. Additionally, in Figure 6b it is observed that high values of GORE are related to high values of NSeff, although, it was not found a direct relation between these two indexes.

In this way, better rainfall estimations produce an improvement in model performance. Similar result was found by Bárdossy and Das (2008) who used 10 and 20 rain gauges for calibration and validation, respectively. Nevertheless, the improvement in the model efficiency was higher in our case. In this way, in a model far from well calibrated any improvement in rainfall input data has the potential to enhance the runoff simulation. Additionally, the fact that bad and good efficiencies can be obtained for the same parameters suggests that for this mountain ecosystem the rainfall input could be the biggest source of model uncertainty.

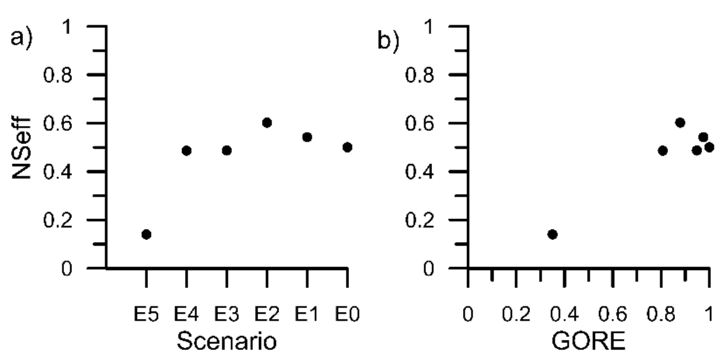

Figure 6: Impact of rainfall quality on model performance (NSeff) of a calibrated model with low rainfall quality against a) rainfall monitoring scenario and b) GORE index.

5. Conclusions

The present study was designed to assess the impact of rainfall estimation on hydrological modelling using six rainfall monitoring scenarios in a small headwater páramo catchment. This was achieved by installing a dense network of 12 rain gauges in the Zhurucay Ecohydrological Observatory in southern Ecuador, and creating rainfall scenarios by withdrawing a given number of rain gauges.

This study identified that all model structures of HBV-light model can represent total runoff. However, the capacity to simulate sub-flow components strongly varied between structures. The simplest structure M1 (standard model) had the highest performance to represent sub-flow components, although all model structures have problems to properly represent slow flow.

The research has also shown that having good spatial rainfall measurements is essential to achieve good modelling results in mountainous areas. We can conclude that a limited number of rain gauges can produce acceptable modelling performances. However, it strongly depends on the location of the rain gauges. In this case, three rain gauges in the upper, middle and lower catchment worked well, but this has to be confirmed in other páramo catchments in order to generalize this knowledge. Furthermore, a better description of the areal rainfall of the catchment not only enhances the runoff simulation but also the possibility to select an optimal parameter value. However, it is still an open question if the sensibility of parameters to the rainfall quality is a function of the number of parameters used by the model.

Another significant finding to emerge from this study is that a calibrated model with far-from-perfect rainfall can produce good or acceptable runoff simulations with new improved rainfall data, something that can be highly valuable by water managers.

The results of this investigation showed that rainfall input could be the largest source of model uncertainty for this mountain ecosystem. Therefore, our findings have provided a first insight of the importance of rainfall monitoring for hydrological modelling in páramo catchments, which are the main water supply for millions of people.

References

Allen, R.G., Pereira, L., Raes, D., Smith, M., 1998. Crop evapotranspiration: Guidelines for computing crop requirements. FAO Irrig. Drain. Pap. No 56. Rome, Italy Food Agric. Organ.

Anctil, F., Lauzon, N., Andréassian, V., Oudin, L., Perrin, C., 2006. Improvement of rainfall-runoff forecasts through mean areal rainfall optimization. J. Hydrol. 328, 717–725. https://doi.org/10.1016/j.jhydrol.2006.01.016

Andréassian, V., Perrin, C., Michel, C., Usart-Sanchez, I., Lavabre, J., 2004. Impact of imperfect rainfall knowledge on the efficiency and parameters of watershed models. J. Hydrol. 250, 206–235. https://doi.org/10.1016/S0022-1694(01)00437-1

Arnaud, P., Bouvier, C., Cisneros, L., Dominguez, R., 2002. Influence of rainfall spatial variability on flood prediction. J. Hydrol. 260, 216–230. https://doi.org/10.1016/S0022-1694(01)00611-4

Arnaud, P., Lavabre, J., Fouchier, C., Diss, S., Javelle, P., 2011. Sensitivity of hydrological models to uncertainty in rainfall input. Hydrol. Sci. J. 56, 397–410. https://doi.org/10.1080/02626667.2011.563742

Avilés, A., Célleri, R., Paredes, J., Solera, A., 2015. Evaluation of Markov chain based drought forecasts in an Andean regulated river basin using the skill scores RPS and GMSS. Water Resour Manag. 29, 1949–1963. https://doi.org/10.1007/s11269-015-0921-2

Avilés, A., Célleri, R., Solera, A., Paredes, J., 2016. Probabilistic forecasting of drought events using Markov chain- and Bayesian network-based models: A case study of an Andean regulated river basin. Water 8, 37. https://doi.org/10.3390/w8020037

Bárdossy, A., Das, T., 2008. Influence of rainfall observation network on model calibration and application. Hydrol. Earth Syst. Sci. 12, 77–89.

Bergström, S., 1992. The HBV Model: Its Structure and Applications. Swedish Meteorol. Hydrol. Inst. (SMHI), Hydrol.

Bergström, S., 1976. Development and application of a conceptual runoff model for Scandinavian catchments. SMHI, Rep. No. RHO 7.

Berne, A., Delrieu, G., Creutin, J.-D., Obled, C., 2004. Temporal and spatial resolution of rainfall measurements required for urban hydrology. J. Hydrol. 299, 166–179. https://doi.org/10.1016/j.jhydrol.2004.08.002

Beven, K., Homberger, G.M., 1982. Assessing the effect of spatial pattern of precipitation in modeling stream flow hydrographs. Water Resour. Bull. 18, 823–829. https://doi.org/10.1111/j.1752-1688.1982.tb00078.x

Buytaert, W., Beven, K., 2011. Models as multiple working hypotheses: Hydrological simulation of tropical alpine wetlands. Hydrol. Process. 25, 1784–1799. https://doi.org/10.1002/hyp.7936

Buytaert, W., Célleri, R., Willems, P., De Bièvre, B., Wyseure, G., 2006a. Spatial and temporal rainfall variability in mountainous areas: A case study from the south Ecuadorian Andes. J. Hydrol. 329, 413–421. https://doi.org/10.1016/j.jhydrol.2006.02.031

Buytaert, W., De Bièvre, B., 2012. Water for cities: The impact of climate change and demographic growth in the tropical Andes. Water Resour. Res. 48, W08503. https://doi.org/10.1029/2011WR011755

Buytaert, W., De Bièvre, B., Wyseure, G., Deckers, J., 2004. The use of the linear reservoir concept to quantify the impact of changes in land use on the hydrology of catchments in the Andes. Hydrol. Earth Syst. Sci. 8, 108–114.

Buytaert, W., Deckers, J., Wyseure, G., 2006b. Description and classification of nonallophanic Andosols in south Ecuadorian alpine grasslands (páramo). Geomorphology 73, 207–221. https://doi.org/10.1016/j.geomorph.2005.06.012

Buytaert, W., Iñiguez, V., Célleri, R., Wyseure, G., Deckers, J., 2006c. Analysis of the water balance of small páramo catchments in south Ecuador, in: J. Krecek and M. Haigh (Eds.): Environmental Role of Wetlands in Headwaters. Springer, pp. 271–281. https://doi.org/10.1007/1-4020-4228-0_24

Buytaert, W., Wyseure, G., De Bièvre, B., Deckers, J., 2005. The effect of land-use changes on the hydrological behaviour of Histic Andosols in south Ecuador. Hydrol. Process. 19, 3985–3997. https://doi.org/10.1002/hyp.5867

Campozano, L., Célleri, R., Trachte, K., Bendix, J., Samaniego, E., 2016. Rainfall and cloud dynamics in the Andes: A southern Ecuador case study. Adv. Meteorol. https://doi.org/10.1155/2016/3192765

Carrillo-Rojas, G., Silva, B., Córdova, M., Célleri, R., Bendix, J., 2016. Dynamic mapping of evapotranspiration using an energy balance-based model over an Andean páramo catchment of southern Ecuador. Remote Sens. 8, 160. https://doi.org/10.3390/rs8020160

Célleri, R., Feyen, J., 2009. The hydrology of tropical Andean ecosystems: Importance, knowledge status, and perspectives. Mt. Res. Dev. 29, 350–355. https://doi.org/10.1659/mrd.00007

Célleri, R., Willems, P., Buytaert, W., Feyen, J., 2007. Space–time rainfall variability in the Paute basin, Ecuadorian Andes. Hydrol. Process. 21, 3316–3327. https://doi.org/10.1002/hyp.6575

Chang, C.-L., Lo, S.-L., Chen, M.-Y., 2007. Uncertainty in watershed response predictions induced by spatial variability of precipitation. Environ. Monit. Assess. 127, 147–153. https://doi.org/10.1007/s10661-006-9268-8

Chaubey, I., Haan, C.T., Salisbury, J.M., Grunwald, S., 1999. Quantifying model output uncertainty due to spatial variability of rainfall. J. Am. Water Resour. Assoc. 35, 1113–1123. https://doi.org/10.1111/j.1752-1688.1999.tb04198.x

Coltorti, M., Ollier, C.D., 2000. Geomorphic and tectonic evolution of the Ecuadorian Andes. Geomorphology 32, 1–19. https://doi.org/10.1016/S0169-555X(99)00036-7

Córdova, M., Carrillo-Rojas, G., Crespo, P., Wilcox, B., Célleri, R., 2015. Evaluation of the Penman-Monteith (FAO 56 PM) method for calculating reference evapotranspiration using limited data. Application to the wet páramo of southern Ecuador. Mt. Res. Dev. 35, 230–239. https://doi.org/10.1659/mrd-journal-d-14-0024.1

Correa, A., Windhorst, D., Crespo, P., Célleri, R., Feyen, J., Breuer, L., 2016. Continuous versus event based sampling : How many samples are required for deriving general hydrological understanding on Ecuador's páramo region? Hydrol. Process. 30, 4059–4073. https://doi.org/10.1002/hyp.10975

Crespo, P., Célleri, R., Buytaert, W., Feyen, J., Iñiguez, V., Borja, P., De Bièvre, B., 2009. Land use change impacts on the hydrology of wet Andean páramo ecocystems, in: In: Status and Perspectives of Hydrology in Small Basins, IAHS Publ. 336. International Association for Hydrological Sciences, pp. 71–76. https://doi.org/10.13140/2.1.5137.6320

Crespo, P., Feyen, J., Buytaert, W., Bücker, A., Breuer, L., Frede, H.G., Ramírez, M., 2011. Identifying controls of the rainfall-runoff response of small catchments in the tropical Andes (Ecuador). J. Hydrol. 407, 164–174. https://doi.org/10.1016/j.jhydrol.2011.07.021

Crespo, P., Feyen, J., Buytaert, W., Célleri, R., Frede, H.-G., Ramírez, M., Breuer, L., 2012. Development of a conceptual model of the hydrologic response of tropical Andean micro-catchments in southern Ecuador. Hydrol. Earth Syst. Sci. Discuss. 9, 2475–2510. https://doi.org/10.5194/hessd-9-2475-2012

Espinosa, J., Rivera, D., 2016. Variations in water resources availability at the Ecuadorian páramo due to land-use changes. Environ. Earth Sci. 75, 1173. https://doi.org/10.1007/s12665-016-5962-1

Ewen, J., Parkin, G., 1996. Validation of catchment models for predicting land-use and climate change impacts. 1. Method. J. Hydrol. 175, 583–594. https://doi.org/10.1016/S0022-1694(96)80026-6

Faurés, J.-M., Goodrich, D.C., Woolhiser, D.A., Sorooshian, S., 1995. Impact of small-scale spatial rainfall variability on runoff modeling. J. Hydrol. 173, 309–326. https://doi.org/10.1016/0022-1694(95)02704-S

Flores-López, F., Galaitsi, S.E., Escobar, M., Purkey, D., 2016. Modeling of Andean páramo ecosystems' hydrological response to environmental change. Water 8, 94. https://doi.org/10.3390/w8030094

Girons Lopez, M., Seibert, J., 2016. Influence of hydro-meteorological data spatial aggregation on streamflow modelling. J. Hydrol. 541, 1212–1220. https://doi.org/10.1016/j.jhydrol.2016.08.026

Gupta, H. V., Beven, K., Wagener, T., 2006. Model calibration and uncertainty estimation, in: Encyclopedia of Hydrological Sciences. John Wiley & Sons, Ltd, Chichester, UK. https://doi.org/10.1002/0470848944.hsa138

Guzmán, P., Batelaan, O., Huysmans, M., Wyseure, G., 2015. Comparative analysis of baseflow characteristics of two Andean catchments, Ecuador. Hydrol. Process. 29, 3051–3064. https://doi.org/10.1002/hyp.10422

Hrachowitz, M., Weiler, M., 2011. Uncertainty of precipitation estimates caused by sparse gauging networks in a small, mountainous watershed. J. Hydrol. Eng. 16, 460–471. https://doi.org/10.1061/(ASCE)HE.1943-5584.0000331

Klemeš, V., 1986. Operational testing of hydrological simulation models. Hydrol. Sci. J. 31, 13–24. https://doi.org/10.1080/02626668609491024

Krause, P., Boyle, D.P., Bäse, F., 2005. Comparison of different efficiency criteria for hydrological model assessment. Adv. Geosci. 5, 89–97.

Legates, D.R., McCabe Jr., G.J., 1999. Evaluating the use of “goodness of fit” measures in hydrologic and hydroclimatic model validation. Water Resour. Res. 35, 233–241. https://doi.org/10.1029/1998WR900018

Lobligeois, F., Andréassian, V., Perrin, C., Tabary, P., Loumagne, C., 2014. When does higher spatial resolution rainfall information improve streamflow simulation? An evaluation using 3620 flood events. Hydrol. Earth Syst. Sci. 18, 575–594. https://doi.org/10.5194/hess-18-575-2014

Mosquera, G.M., Célleri, R., Lazo, P.X., Vaché, K.B., Perakis, S.S., Crespo, P., 2016a. Combined use of isotopic and hydrometric data to conceptualize ecohydrological processes in a high-elevation tropical ecosystem. Hydrol. Process. 30, 2930–2947. https://doi.org/10.1002/hyp.10927

Mosquera, G.M., Lazo, P.X., Célleri, R., Wilcox, B.P., Crespo, P., 2015. Runoff from tropical alpine grasslands increases with areal extent of wetlands. Catena 125, 120–128. https://doi.org/10.1016/j.catena.2014.10.010

Mosquera, G.M., Segura, C., Vaché, K.B., Windhorst, D., Breuer, L., Crespo, P., 2016b. Insights on the water mean transit time in a high-elevation tropical ecosystem. Hydrol. Earth Syst. Sci. 20, 2987–3004. https://doi.org/10.5194/hess-20-2987-2016

Nash, J.E., Sutcliffe, J. V., 1970. River flow forecasting through conceptual models part I - A discussion of principles. J. Hydrol. 10, 282–290. https://doi.org/10.1016/0022-1694(70)90255-6

Obled, C., Wendling, J., Beven, K., 1994. The sensitivity of hydrological models to spatial rainfall patterns: an evaluation using observed data. J. Hydrol. 159, 305–333. https://doi.org/10.1016/0022-1694(94)90263-1

Ochoa-Tocachi, B.F., Buytaert, W., De Bièvre, B., Célleri, R., Crespo, P., Villacís, M., Llerena, C.A., Acosta, L., Villazón, M., Guallpa, M., Gil-Ríos, J., Fuentes, P., Olaya, D., Viñas, P., Rojas, G., Arias, S., 2016. Impacts of land use on the hydrological response of tropical Andean catchments. Hydrol. Process. 30, 4074–4089. https://doi.org/10.1002/hyp.10980

Padrón, R.S., Wilcox, B.P., Crespo, P., Célleri, R., 2015. Rainfall in the Andean páramo: New insights from high-resolution monitoring in southern Ecuador. J. Hydrometeorol. 16, 985–996. https://doi.org/10.1175/JHM-D-14-0135.1

Pechlivanidis, I.G., McIntyre, N., Wheater, H.S., 2016. The significance of spatial variability of rainfall on runoff: an evaluation based on the Upper Lee catchment,UK. Hydrol. Res. 48, 478–485. https://doi.org/10.2166/nh.2016.038

Pinos, J., Studholme, A., Carabajo, A., Gracia, C., 2016. Leaf litterfall and decomposition of polylepis reticulata in the treeline of the Ecuadorian Andes. Mt. Res. Dev. 37, 87–96. https://doi.org/10.1659/MRD-JOURNAL-D-16-00004.1

Plesca, I., Timbe, E., Exbrayat, J.-F., Windhorst, D., Kraft, P., Crespo, P., Vaché, K.B., Frede, H.-G., Breuer, L., 2012. Model intercomparison to explore catchment functioning: Results from a remote montane tropical rainforest. Ecol. Modell. 239, 3–13. https://doi.org/10.1016/j.ecolmodel.2011.05.005

Quichimbo, P., Tenorio, G., Borja, P., Cárdenas, I., Crespo, P., Célleri, R., 2012. Efectos sobre las propiedades físicas y químicas de los suelos por el cambio de la cobertura vegetal y uso del suelo: Páramo de Quimsacocha al sur del Ecuador. Suelos Ecuatoriales 42, 138–153.

Ramsay, P.M., Oxley, E.R.B., 1997. The growth form composition of plant communities in the Ecuadorian paramos. Plant Ecol. 131, 173–192. https://doi.org/10.1023/A:1009796224479

Sarmiento, G., 1986. Ecologically crucial features of climate in high tropical mountains. F. Vuilleumier, M. Monast. (Eds.), High Alt. Trop. Biogeogr. Oxford Univ. Press. Oxford 11–45.

Sarmiento, L., 2000. Water balance and soil loss under long fallow agriculture in the Venezuelan Andes. Mt. Res. Dev. 20, 246–253. https://doi.org/10.1659/0276-4741(2000)020[0246:WBASLU]2.0.CO;2

Sarmiento, L., Llambí, L.D., Escalona, A., Marquez, N., 2003. Vegetation patterns, regeneration rates and divergence in an old-field succession of the high tropical Andes. Plant Ecol. 166, 145–156. https://doi.org/10.1023/A:1023262724696

Segond, M.-L., Wheater, H.S., Onof, C., 2007. The significance of spatial rainfall representation for flood runoff estimation: A numerical evaluation based on the Lee catchment , UK. J. Hydrol. 347, 116–131. https://doi.org/10.1016/j.jhydrol.2007.09.040

Seibert, J., 1999. Regionalisation of parameters for a conceptual rainfall-runoff model. Agric. For. Meteorol. 98–99, 279–293. https://doi.org/10.1016/S0168-1923(99)00105-7

Seibert, J., 1997. Estimation of parameter uncertainty in the HBV model. Nord. Hydrol. 28, 247–262.

Seibert, J., Vis, M.J.P., 2012. Teaching hydrological modeling with a user-friendly catchment-runoff-model software package. Hydrol. Earth Syst. Sci. 16, 3315–3325. https://doi.org/10.5194/hess-16-3315-2012

Singh, V.P., 1997. Effect of spatial and temporal variability in rainfall and watershed characteristics on stream flow hydrograph. Hydrol. Process. 11, 1649–1669. https://doi.org/10.1002/(SICI)1099-1085(19971015)11:12<1649::AID-

HYP495>3.0.CO;2-1

Sklenář, P., Jørgensen, P.M., 1999. Distribution patterns of paramo plants in Ecuador. J. Biogeogr. 26, 681–691. https://doi.org/10.1046/j.1365-2699.1999.00324.x

Steele-Dunne, S., Lynch, P., Mcgrath, R., Semmler, T., Wang, S., Hanafin, J., Nolan, P., 2008. The impacts of climate change on hydrology in Ireland. J. Hydrol. 356, 28–45. https://doi.org/10.1016/j.jhydrol.2008.03.025

Syed, K.H., Goodrich, D.C., Myers, D.E., Sorooshian, S., 2003. Spatial characteristics of thunderstorm rainfall fields and their relation to runoff. J. Hydrol. 271, 1–21. https://doi.org/10.1016/S0022-1694(02)00311-6

Uhlenbrook, S., Seibert, J., Rodhe, A., 1999. Prediction uncertainty of conceptual rainfall-runoff models caused by problems in identifying model parameters and structure. Hydrol. Sci. J. 44, 779–797. https://doi.org/10.1080/02626669909492273

Viviroli, D., Du, H.H., Messerli, B., Meybeck, M., Weingartner, R., 2007. Mountains of the world, water towers for humanity: Typology, mapping, and global significance. Water Resour. Res. 43, W07447. https://doi.org/10.1029/2006WR005653

Willems, P., 2009. A time series tool to support the multi-criteria performance evaluation of rainfall-runoff models. Environ. Model. Softw. 24, 311–321. https://doi.org/10.1016/j.envsoft.2008.09.005

Xu, H., Xu, C.-Y., Chen, H., Zhang, Z., Li, L., 2013. Assessing the influence of rain gauge density and distribution on hydrological model performance in a humid region of China. J. Hydrol. 505, 1–12. https://doi.org/10.1016/j.jhydrol.2013.09.004

Younger, P.M., Freer, J.E., Beven, K., 2009. Detecting the effects of spatial variability of rainfall on hydrological modelling within an uncertainty analysis framework. Hydrol. Process. 23, 1988–2003. https://doi.org/10.1002/hyp.7341